Pattern Recognition Letters 2 (1983) 117–123
North-Holland

December 1983

The application of image analysis techniques to mineral processing

Ting-Chuen PONG[1], Robert M. HARALICK[1],
James R. CRAIG[2],
Roe-Hoan YOON[3], Woo-Zin CHOI[3]

Spatial Data Analysis Laboratory, Departments of [1]Computer Sciences, [2]Geological Sciences, and [3]Mining and Minerals Engineering, Virginia Polytechic Institute and State University, Blacksburg, VA 24061, USA

Received 10 March 1983
Revised 1 September 1983

Abstract: With the increasing demand for minerals, the development of efficient techniques for mineral recovery is important. The application of image analysis techniques to mineral beneficiation studies is described in this paper. We carry out ore identification not pixel-by-pixel but rather by considering the average reflectance of grains. This is accomplished by first carrying out segmentation, a process in which a facet model based edge operator is used to delineate the boundaries of grains.

Key words: Image analysis, mineral benefication.

1. Introduction

The increasing demand for mineral resources, the increasing dependence on lower grade resources, and the increasing costs of energy necessitate the development of new, and the streamlining of old techniques in the mineral industry. Image analysis techniques which have already been found useful in research areas such as biomedical applications, industrial automation and remote sensing, are just beginning to find applications in the mineral processing industry. The present paper describes the application of image analysis techniques to the characterization and analysis of mineral beneficiation products.

Petruk (1976) of the Canada Center for Minerals and Energy Technology (CANMET) describes the application of the Quanitimet image analyser to quantitative mineralogical analysis. In 1978, a Leitz–T.A.S. automatic image analyser was installed in the Mineralogy Division of the National Institute for Metallurgy in South Africa. A general description of the system is given by Oosthuyzen (1980).

Grains can generally be differentiated on the basis of their differing reflectances. In most commercial machines presently operational, a threshold decision on reflectances is made on a pixel-by-pixel basis depending upon their reflectance. This technique is highly susceptable to the noise of the random variations inherent in the grains, thereby making area counts of grains having similar but different reflectances subject to inaccuracies. In contrast, the approach we suggest here first segments the image using an edge operator to delineate the boundary of the grain. To identify the grain we use the average reflectance of all pixels surrounded by the edges. Section 2 describes the entire grain identification process which starts from the low level image preparation and image segmentation steps to the higher level property extraction and grain classification process.

0167-8655/83/$3.00

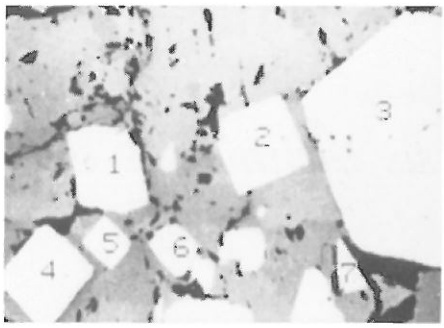

Fig. 1. An example of a digitized image of pyrrhotite-pyrite ore.

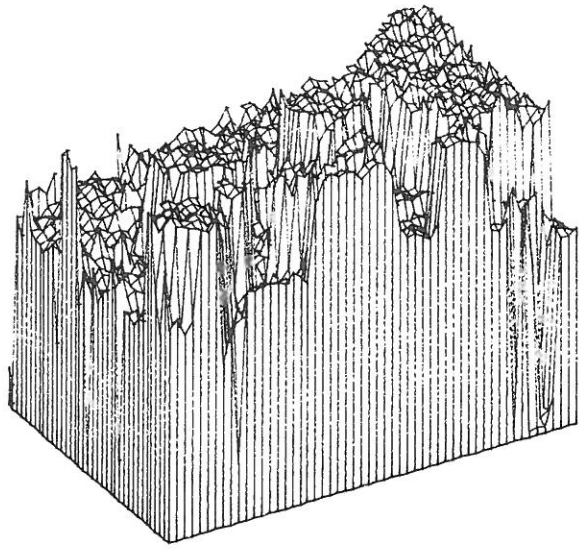

Fig. 2a. The surface plot of the image of Figure 1 in which the surface irregularity indicates the variations in the reflectance.

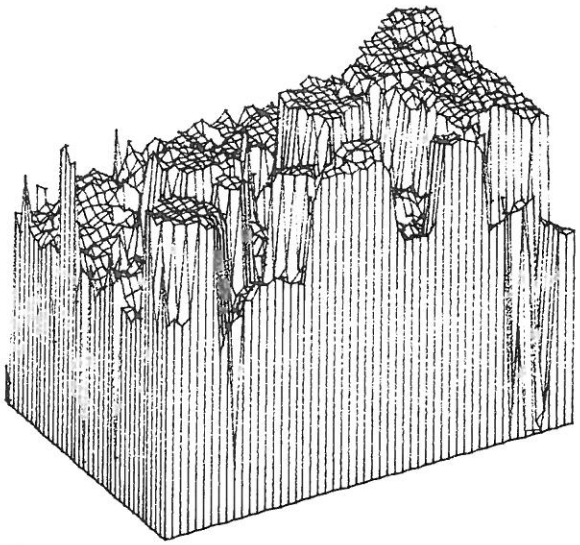

Fig. 2b. The surface plot of the smoothed image of the image of Figure 1.

2. Processing of mineral images

2.1. Image preparation

Most ore minerals are opaque and hence are studied by means of reflected light microscopy. Samples were cut, ground and polished according to the procedures described by Craig and Vaughan (1981). In our system, ore images are either generated directly from a Hamamatsu C-1000 television camera mounted on a Leitz Orthoplan microscope or digitized from a 35mm film negative by a laser scanner. The size of the image generated by the television camera can be as large as 512×512 pixels, while the laser scanner can produce a 1000×1000 image from a 35mm negative. The individual pixels each have a reflectance (or grey tone inensity) which is proportional to the composite reflection coefficient of the ore sample at the corresponding spatial location in the sample.

Images generated by these methods are subject to noise. Our methodology includes noise removal operations such as median filter, box filter and peak noise removal to remove these undesirable features from the image. This reduces the occurrence of error in later processing. Figure 1 shows an example of a digitized image (256×256). Figures 2a and 2b show the surface plots of the original image and the smoothed image respectively.

2.2. Edge detection

The facet model is used to accomplish the step edge detection which is required in our segmentation process. A precise mathematical description of the edge operator can be found in Haralick (1982, 1983). The facet model states that any analysis made on the basis of the pixel values in some neighborhood has its final authoritative interpretation relative to the underlying grey tone intensity surface and that the neighborhood pixel values are noisy sampled observations of the underlying surface.

Pixels which are part of regions have simple grey tone intensity surfaces over their areas. Pixels which have an edge in them have complex grey tone intensity surfaces over their areas. Specifically, an edge occurs in a pixel if and only if there

is some point in the pixel's area having a zero crossing of the second directional derivative taken in the direction of a non-zero gradient at the pixel's center.

To determine whether or not a pixel should be marked as a step edge pixel, its underlying grey tone intensity surface must be estimated on the basis of the pixel values in its neighborhood. For this, we use a least squares fit with a functional form consisting of a linear combination of the tensor products of discrete orthogonal polynomials. The highest order tensor product we currently use is cubic (i.e. the highest order terms are x^3, x^2y, xy^2 and y^3). The appropriate directional derivatives are easily computed from this kind of a function. By using a 7×7 neighborhood, Figure 3 shows the detected edges of the image of Figure 1.

2.3. Region extraction

Once edge pixels have been marked by the edge operator, the regions extracted are the largest connected areas of pixels which are entirely surrounded by edge pixels. This process is accomplished by a connected components algorithm which assigns a unique label to each maximally connected group of non-edge pixels. An efficient memory limited connected components algorithm is implemented and its validity is proved (Lumia (1982)). This algorithm requires only one top-down scan and one bottom-up scan of the entire image.

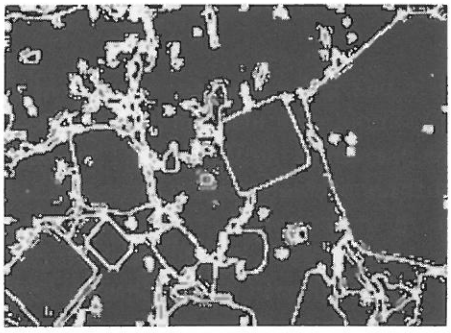

Fig. 3. An example of the edge image of the image of Figure 1.

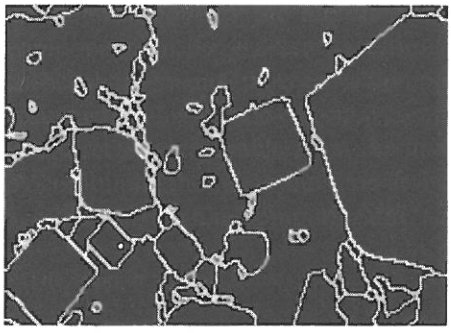

Fig. 4. The resulting segmentation of the image of Figure 1. The minimum size of individual segments is 10 pixels.

After the non-edge pixels have been labelled, the edge pixels which exist between regions will stay unaffected. If a more accurate area count of grains is desired, a symmetric fill operator can be used to fill up all or part of these gaps by expanding the regions. Experiments show that polished effects at grain bondaries and internal imperfections (due to scratches, inclusions, etc.) often create a large number of small regions. These regions will lead to an inaccurate count of grains and to misclassification of grains. In order to avoid these problems, small regions with sizes less than a certain size threshold are first marked and then eliminated by expanding symmetrically the neighboring unmarked regions. By eliminating all regions with less than ten pixels, the resulting segmentation of the image of Figure 1 is illustrated in Figure 4.

The region extraction process, though working well for most images, sometimes produces opened regions when the detected edges are unable to close the boundaries of grains. In these cases, the edges are expanded symmetrically for a few pixels or until the gaps are closed. The expanded edges are then shrunk by expanding the labelled regions after the connected components step.

2.4. Region property list

Once an image has been segmented into regions, properties of the regions ae computed. Currently, as many as thirty measurements are kept for each region. Among the set of properties measured for each region, the following measurements are most useful in mineralogical analysis.

(1) *Area* and *perimeter* of a region. They are measured respectively as the number of pixels in a region and the number of boundary pixels of a region.

(2) *Grey level information* consists of the four grey level region properties: maximum, minimum, mean and variance.

(3) The *center of mass* $(\bar{x}, \bar{y})$ of a region. It gives the spatial distribution of the regions in the image.

(4) *Elongation* and *angle* are measures of the shape and orientation of a figure. Elongation is obtained as the ratio of the length of the major axis to the length of the minor axis of the best fitting ellipse of the region. Angle is measured as the slope of the major axis of the best fitting ellipse.

(5) The *ellipticity measure* satisfies the following criteria:

1. it increases as a figure becomes more circular;
2. the results for digital figures follow those for the corresponding continuous figures;
3. it is orientation independent; and
4. it is size independent.

Haralick (1975) shows that the ratio of the mean u_r to the standard deviation s_r of the distances from the center of the figure to its boundary points has these properties. We calculate ellipticity after rotating and scaling the region so that its best fitting ellipse becomes a circle. This is done to separate the effect of elongation from ellipticity. For a region R centered at $(\bar{x}, \bar{y})$, the radius of a boundary point (x, y) of R is computed as:

$$r = [e * ((x-\bar{x})\sin\theta + (y-\bar{y})\cos\theta)^2 + ((x-\bar{x})\cos\theta - (y-\bar{y})\sin\theta)^2]^{1/2}$$

where e and θ are elongation and angle respectively. And the ellipticity measure C_R is given by:

$$C_R = \frac{s_r}{u_r}.$$

2.5. Grain classification

After the segmentation process, each region in the segmented image is tagged with a unique label. A region property file which contains for each region in the segmented image a set of properties is also generated. The individual regions can then be classified on the basis of their average grey intensities, which are stored in the property file. The results of classification are then written back into some designated areas of the property file.

A training phase is required in order to obtain the parameters necessary for classifying grains of different types. In the training phase, ore samples of known reflectances are prepared and input to the computer as training images. From a training image we generate a segmented image and a corresponding region property file. The operator can then identify, with the aid of an interactive display, all the grains of a particular type. A simple decision rule, which is usually based on the average grey intensities of the segments of the known grains, is then obtained and entered into the system and is used to identify grains in unknown samples.

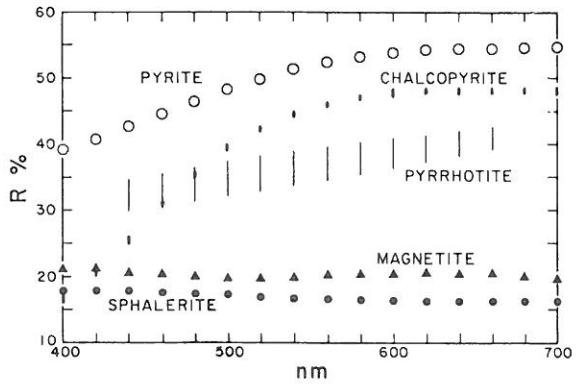

Fig. 5. Reflectance curves for the common ore minerals encountered in massive sulfide ores of the Central and Southern Appalachians. Data are taken from Henry (1977).

The above classification process relies upon the differences in reflectances to separate one phase from another. Such separation is readily accomplished if there are broad differences between the reflectances but becomes difficult if the reflectance differences are small and/or variable (e.g. due to differences in polishing, in bireflectance, or high density of inclusions of fracures). Figure 5 illustrates the reflectance curves for pyrite, pyrrhotite, chalcopyrite, magnetite and sphalerite from 400 nm to 700 nm. The distinct differences between pyrite, pyrrhotite, and magnetite at all wavelengths are apparent; these differences allow for relatively easy discrimination in reasonably well polished samples. The reflectance curve for chalcopyrite lies below that for pyrrhotite at wavelengths less than 460 nm but above the pyrrhotite curve at wavelengths above about 500 nm. It is known that chalcopyrite, although distinct to the human eye because of its yellow color, is difficult for image analysis systems (operating in black and white) to separate from pyrrhotite because the reflectances are similar when averaged across the white light

spectrum. The present investigators found that if monochromatic light in the ranges 440–460 nm or 560–620 nm were used for illumination, phase separation of pyrrhotite and chalcopyrite should be most readily accomplished.

Although mineralogic identification is generally accomplished by means of differences in reflectance (grey-level), our system also allows identification on the basis of size, shape, surface texture or color from multi-band images.

3. Applications to mineral processing

3.1. Liberation studies

The 'degree of liberation' is a measure of the degree to which mineral particles occur as individual singlephase units in a crushed sample. Determination of the degree of liberation of each type of mineral species in beneficiation is vital in mineral processing. The degree of liberation (L_i) of mineral component i can be determined by the following formula:

$$L_i = 100 \times \frac{A_i^F}{A_i^F + f_i A_i^L}$$

where A_i^F is the total area of mineralogical component i occurring as free particles, A_i^L is the total area of mineralogical component i occurring as locked particles, and f_i is the locking factor of the mineral. A region is considered to be locked if it is adjacent to any other non-background region of different type, and is considered to be free otherwise.

To accomplish the liberation computation, a region adjacency graph must be determined. The region adjacency graph contains indexes of all pairs of adjacent regions in the segmented image. Two regions R_1 and R_2 are said to be *adjacent* if there exists some pixel in R_1 having a neighboring pixel in R_2. Once a region adjacency graph is obtained, locked and free particles can easily be determined by comparing the mineral types of pairs of adjacent regions from the adjacency graph.

In addition to the degree of liberation, the following cooccurrence measurements can also be obtained from the region property list and the region adjacency graph: (1) the percentage of a phase which occurs as locked particles; (2) the percentage of particles which are locked; and (3) the correlation of each mineral species with each other mineral species.

3.2. Shape analysis

Mineralogical shape in an ore or rock is a function of the growth characteristics of the mineral (i.e. some minerals such as pyrite and garnet have a strong 'force of crystallization' and characteristically assume euhedral shapes), the environment of initial formation (i.e. open voids vs. crystallizing melts, etc.), and their post-depositional history (i.e. recrystallization or fracturing due to metamorphism). The shape of the mineral grain may in turn affect the manner in which it responds to crushing, grinding, and liberation. We currently allow the quantitative determination of particle shape in terms of elongation and circularity. Examples of elongation and cirularity measurements are demonstrated for ideal shapes and for real grain in complex sulfide ores in Figure 6 and Figure 1.

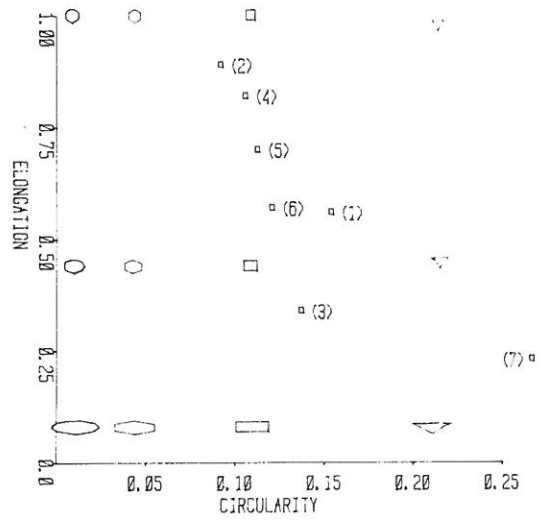

Fig. 6. The circularity and elongation measures for ideal and real figures. The real figures correspond to the numbered grains of Figure 1.

3.3. Areal and grain size distributions

The mineralogical composition of an ore or benefication product is measured in terms of the

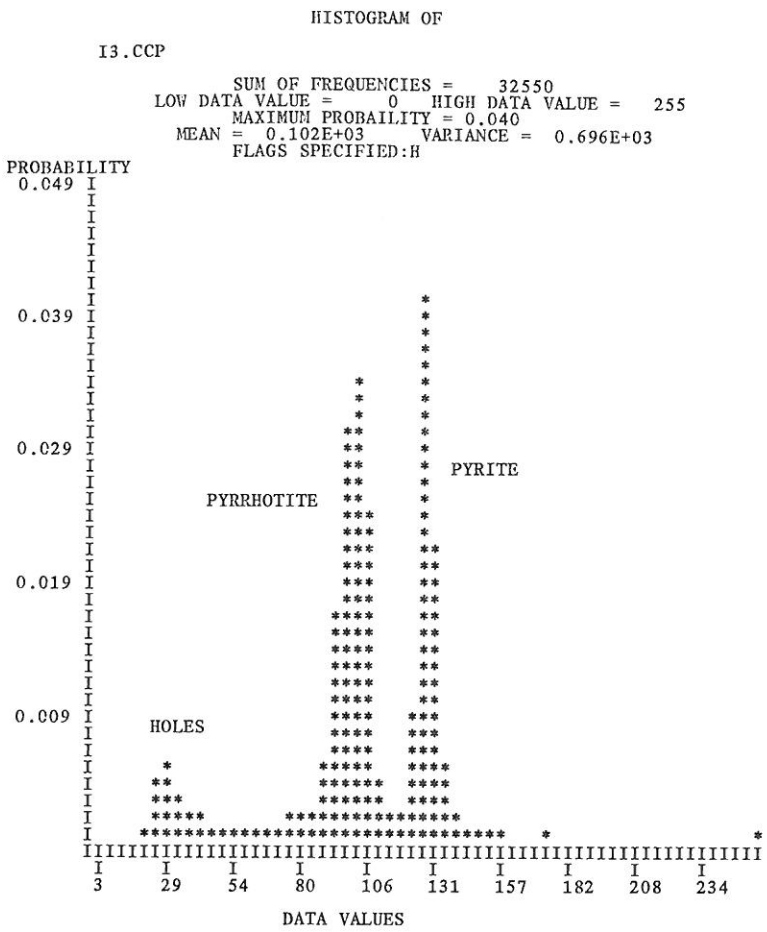

Fig. 7. The histogram of the mineralogical content of the image in Figure 1 in terms of reflectance.

area occupied by each mineral in a polished section or thin section. Figure 7 represents a typical histogram of mineral reflectance versus abundance for the image shown in Figure 1; once limits are specified, the calculation of areal percentages of each phase is immediate.

Measurements of the sizes of the individual mineral grains and/or the distributions of grain sizes in samples are extremely important, because the sizes determine the degree of liberation of minerals during beneficiation. Knowledge of the size distribution therefore allows for prediction of liberation characteristics and the use of minimal amounts of energy during comminution.

4. Concluding remarks

We have described in this paper the application of image processing techniques to mineral beneficiation studies. The success of our work will help the mineral industry in recovering base metal efficiently from the domestic fine-grained ore deposits. Furthermore, the basic knowledge gained in this work is hoped to benefit the other application areas in image processing.

References

Craig, J.R. and D.J. Vaughan (1981). *Ore Microscopy and Ore Petrography.* Wiley Interscience, New York.

Haralick, R.M. (1975). A measure of circularity of digital figures. *IEEE Trans. Systems Man Cybernet.* 5, 394–396.

Haralick, R.M. (1982). Zero-crossing of second directional derivative edge operator. *SPIE Proceedings on Robot Vision,* Arlington, VA.

Haralick, R.M. (1983). The digital step edge, *IEEE Trans. Pattern Anal. Mach. Intell.*, to appear.

Henry, N.F.M., Editor (1977). *IMA/COM Quantitative Data File,* Commission on Ore Microscopy, Applied Mineralogy Group, Mineralogical Society, London.

Lumia, R. (1982). A new connected components algorithm for virtual memory computers. *Proceedings IEEE Conference on Pattern Recognition and Image Processing,* 560–565.

Oosthuyzen, E.J. (1980). An elementary introduction to image analysis – a new field of interest at the National Institute for Metallurgy. NIM Report No. 2058, South Africa.

Petruk, W. (1976). The application of quantitative mineralogical analysis of ores to ore dressing. *C.I.M. Bull.* 69, 146–153.